Proceedings of the 33rd
Conference on Decision and Control
Lake Buena Vista, FL - December 1994

WP-4 3:50

Identification and $\mathcal{H}_\infty$ Control Design for a Pressurized Water Reactor

Pascale Bendotti and Bobby Bodenheimer
pascale@hot.caltech.edu bobby@hot.caltech.edu
Electrical Engineering, 116-81
California Institute of Technology
Pasadena, CA 91125

Abstract

The objective of this paper was to design controllers for a Pressurized Water Reactor using model based control techniques. To this end, the physical system was identified from experimental data using a multi-input multi-output state-space description; an $\mathcal{H}_\infty$ controller was designed using a lower order model of the plant. Of particular importance, the frequency weighting functions were chosen to reflect the robust stability and nominal performance requirements. Although a nonlinear controller is required, the results demonstrate the effectiveness of the proposed controller in a relatively wide operating range.

1 Introduction

Most nuclear power plants are Pressurized Water Reactors (PWR). Moreover, in France and in some other countries the major contribution to electricity production is provided by nuclear power. Therefore, nuclear power plants have to provide on-line the required amount of energy. This energy is time-varying, which was not the objective of the controllers originally implemented for the control of the PWR. Due to the change in the specifications, the control system needs to be redesigned, with model-based control techniques.

The first problem addressed in this paper is the identification of a multi-input multi-output model which captures the main dynamical features of the plant, with the condition that the identified model should be reasonably simple and should minimally cover the experimental data set. Due to the complex nature of the actual physical system, the linear time-invariant model identified experimentally cannot predict the real system's dynamical behavior. Recent work in feedback synthesis theory has bred methodologies which result in controllers with a guaranteed robustness and performance for a given mathematical model of a physical system. For these guarantees to also hold on the actual system, a robust control design methodology is needed, that takes the discrepancies between the physical and mathematical model into account. This leads to the second problem addressed in this paper. An $\mathcal{H}_\infty$ methodology is used to design the controller. Using a similar approach, previous results have been obtained with an $\mathcal{H}_2$ controller [1].

In the following sections of this paper, the control approach employed is presented in distinct steps: problem statement, system identification, design model, uncertainty description, performance specifications and $\mathcal{H}_\infty$ control design.

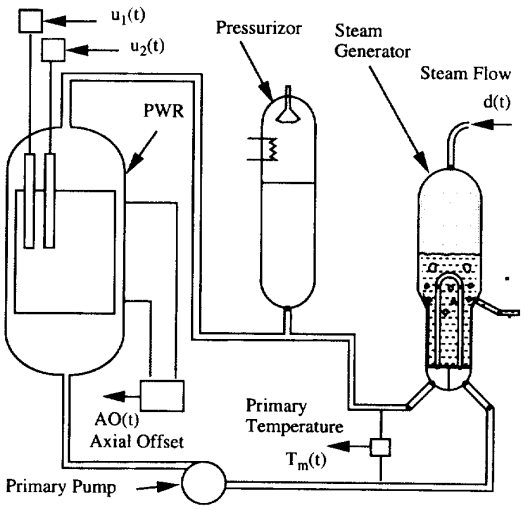

Figure 1: Primary Circuit and Steam Generator

2 Problem Statement

The main objective in controlling a PWR is to provide the commanded power while respecting physical constraints. Consider the application depicted in Figure 1. The pressurized water in the primary circuit transmits the heat generated by the nuclear reaction to the steam generator. In the steam generator, water of the secondary circuit turns into hot steam which drives a turbo-alternator to generate electricity. The rate of the reaction is controlled by control rods. The rods capture neutrons thus slowing down the nuclear reaction; withdrawing them increases the reaction.

From a PWR control standpoint, the required power corresponds to a specific steam flow input that may be viewed as a measurable disturbance. A natural control objective is to track a temperature reference derived from the steam flow. Because of the way in which the control rods enter the reactor, the rate of reaction is always higher at the bottom of the reactor. The axial offset is defined as the difference in power generated between the top and the bottom of the PWR. Safety specifications require the minimization of the axial offset. To achieve such objectives, two inputs are available to control the rates of motion of the control rods, called u_1 and u_2. The vertical positions of the control rods are measured and will be denoted v_1 and v_2. The physics of the reactor make it so u_2 has more authority than u_1 at lower power, and using it results in a smaller axial off-

0-7803-1968-0/94$4.00©1994 IEEE

set. At high power, however, u_2 has almost no authority, so all control must come from u_1.

The actual control strategy is not multivariable, but is a two-step procedure. First, the second input is a nonlinear multiple of the required power, implemented in a feed-forward manner. Second, the PWR temperature is controlled using the first control input u_1 with a nonlinear PID controller. The axial offset is not explicitly taken into account in this control strategy. In particular, the measurement of the axial offset is not used. A multivariable controller is needed to deal with the above shortcomings. However, as the proposed controller is linear, some limitations on achievable performances depending on the operating conditions are expected.

3 System Identification

System identification is a necessary part of any model based control design. From an identification point of view, the problem is to demonstrate that a complex system can be represented by a MIMO state-space description of relatively low order.

3.1 Identification Experiments

In the present case, the identification experiments have been carried out using a realistic nonlinear simulator developed at Electricite de France (EDF). As the model of the simulator is based on partial differential equations, it cannot be represented completely over all frequencies by a finite-dimensional model. The experimental planning should therefore be set up such so major dynamic components are captured in a given frequency range.

The system possesses nonlinearties of two types. The first depends on the operating condition and hence is strongly related to the commanded power. No *a priori* knowledge can be used in the identification process for this type of nonlinearity, so the experimental data are obtained around different operating points, and the resulting model is a linearization at the operating point. The second nonlinearity is on the input magnitude of v_2: this control becomes ineffective when the commanded power tends to its maximum. This maximal value is usually referred to as the nominal power of the plant, P_n. The static characteristic of the input effectiveness is actually known *a priori*, so its inversion allows identification close to the nominal power, where the nonlinear effect is maximal.

3.2 MIMO State-space Description

Consider the system depicted in Figure 2, where T_m, AO, P_I, d, v_1 and v_2 are the temperature, the axial offset, the power, the steam flow and the vertical positions of the rods, respectively.

The physical system is described by a linear time-invariant (LTI) system around an operating point given by the following:

$$x(t+1) = Ax(t) + Bv(t) + \Gamma d(t) \quad (1)$$

$$y_s(t) = Cx(t) + Dv(t) \quad (2)$$

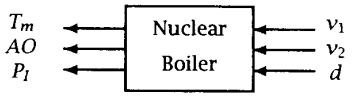

Figure 2: Plant System

with

$$y_s(t) = \begin{pmatrix} T_m(t) \\ AO(t) \\ P_I(t) \end{pmatrix} \text{ and } v(t) = \begin{pmatrix} v_1(t) \\ v_2(t) \end{pmatrix}$$

where $x(t), y_s(t), v(t)$ and $d(t)$ represent the state, the output, the input and the disturbance, respectively, at time t. The parameters of the state-space realization consist of the elements of the A, B, C, D and Γ matrices.

Since the number of parameters rises quadratically with the state dimension, there are a large number of them in a state-space realization. To meaningfully reduce them, specific realizations are used where some parameters are fixed at either zero or one, for example, the well known MIMO canonical forms. Unfortunately, these realizations still contain too many parameters to be uniquely identified.

Re-parameterizing the realizations using physical considerations can overcome this problem. Preliminary identification of several SISO and MISO transfer functions are performed to provide insight into an appropriate re-parameterization (cf. References in [2]). Indeed, the primary temperature and power are mainly related to the control inputs by a second and first order system, respectively. Furthermore, the inputs affect the plant dynamics in an identical manner, although the gains are different. The axial offset is almost a linear combination of the inputs: thus no states are needed for it. These insights provide an appropriate identification-oriented state-space realization structure. Hence, only the temperature and the power have dynamics. The effect of the disturbance has a larger delay than the effect of the control and hence the dimension of the state must reflect this. More precisely, 3 delay values for each of temperature and power (instead of 2 and 1, respectively, in the disturbance-free case) are required to appropriately predict the input-output behavior. This leads to a sixth order state-space realization defined as follows:

$$A = \begin{pmatrix} 0 & 1 & 0 & 0 & 0 & 0 \\ 0 & 0 & 1 & 0 & 0 & 0 \\ a_1^{11} & a_2^{11} & a_3^{11} & 0 & a_2^{12} & 0 \\ 0 & 0 & 0 & 0 & 1 & 0 \\ 0 & 0 & 0 & 0 & 0 & 1 \\ a_1^{21} & 0 & 0 & a_1^{22} & a_2^{22} & a_3^{22} \end{pmatrix}$$

$$B = \begin{pmatrix} b_1^1 & b_2^1 \\ 0 & 0 \\ 0 & 0 \\ 0 & 0 \\ 0 & 0 \\ 0 & 0 \end{pmatrix}, \Gamma = \begin{pmatrix} 0 \\ 0 \\ \gamma_3 \\ 0 \\ 0 \\ \gamma_6 \end{pmatrix} \quad (3)$$

$$C = \begin{pmatrix} 1 & 0 & 0 & 0 & 0 & 0 \\ 0 & c_2^2 & 0 & c_4^2 & 0 & 0 \\ 0 & 0 & 0 & 1 & 0 & 0 \end{pmatrix}, D = \begin{pmatrix} 0 & 0 \\ d_2^1 & d_2^2 \\ d_3^1 & d_3^2 \end{pmatrix}$$

The state matrix A can be partitioned as follows:

$$A = \begin{pmatrix} A_{11} & A_{12} \\ A_{21} & A_{22} \end{pmatrix}$$

where A_{11} and A_{22} denote the third order systems for the temperature and the power; A_{12} and A_{21} represent the cross coupling matrices, which contain only one non-zero term, appropriately located. The input matrix B accounts for the actual delayed effect of the control inputs on primary temperature and power, so only the first row of B has non-zero elements. Similarly, the delay between the control inputs and the disturbance can be taken into account using only the third and sixth elements of the disturbance input matrix Γ. The second row of the output matrix C adds memory to the axial offset. Finally, the elements of D correspond to the direct terms appearing in the axial offset and the power. This results in a specific identification-oriented realization with 18 parameters, instead of the 28 parameters in the standard canonical form.

3.3 MIMO Identification

Similarly, the overall system (1)-(2) can also be modeled by the transfer function:

$$y_s(t) = G_v(\theta, q)v(t) + G_d(\theta, q)d(t) \qquad (4)$$

where q denotes the standard forward shift operator (the corresponding z operator will be omitted for simplicity), and θ represents the vector of free parameters to be identified.

Given a description (4) properly parameterized by the specific form (3) and the input-output data v, y_s and d, the prediction error e is computed as follows:

$$e(t) = y_s(t) - G_v(\theta, q)v(t) - G_d(\theta, q)d(t)$$

For multi-output systems, the identification method consists in determining the parameter estimates by minimizing the following quadratic criterion:

$$\hat{\theta} = \arg\min_{\theta} \det \left[\frac{1}{N} \sum_{i=1}^{N} e(t)e^T(t) \right]$$

using an iterative Gauss-Newton algorithm [3].

3.4 Validation and Results

Finally, to check the ability of the identified model to predict the behavior of the physical system around a specific operating point, the model was validated on a different data set from the one with which it was estimated. Such a procedure was successful over a large operating range due to the static inversion performed at the plant input. In particular, the specific form used for the parameterization was validated.

The time-domain responses of the identified model obtained around $50\%P_n$ (dashed) are plotted against the experimental data (continuous) in Figure 3. The inputs v_1 (continuous), v_2 (dashed) and d (dotted) are plotted in the right lower diagram in Figure 3. The step-responses of the identified models obtained around $50\%P_n$, $90\%P_n$ and $99\%P_n$, called $\hat{G}_0$, $\hat{G}_1$, and $\hat{G}_2$, respectively, are shown in Figure 4.

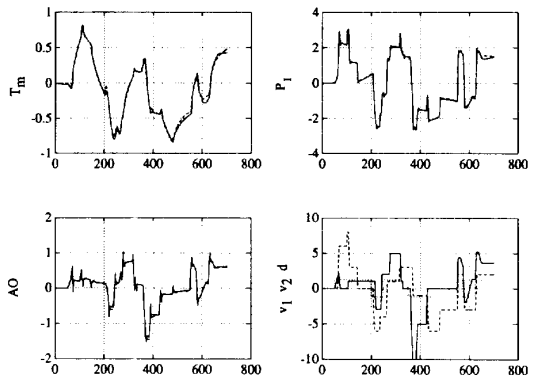

Figure 3: Experimental Data versus Time-domain responses of $\hat{G}_0$

4 Control Design

The controller is designed using an $\mathcal{H}_\infty$ methodology. $\mathcal{H}_\infty$ synthesis is aimed at disturbance rejection. A tracking problem such as the PWR can be cast as disturbance rejection by rejecting the low frequency components of the error between plant output and the reference. As the synthesis is in continuous time, the weighting functions are specified in continuous time as well. Then the discrete time $\mathcal{H}_\infty$ controller is obtained using the bilinear transformation.

4.1 Design Model

From a design point of view, lower order plant models result in lower order controllers, as most popular optimal control strategies (LQG, $\mathcal{H}_2$, $\mathcal{H}_\infty$) yield controllers with state dimension equal to that of the open-loop plant. It is often desirable to obtain a reduced order model as an approximation of the high order model, in the present case the sixth order MIMO model. A balanced realization technique (Moore [4]), including specified model reduction weightings, is used [5].

In particular, dynamic behavior at high frequencies can be considered uncertainty. Therefore, the measurements are weighted with low-pass filters to attenuate the high frequency dynamics. Finally, the reduced order model is obtained by truncating weakly controllable and observable states. The resulting MIMO reduced order plant model is first order, i.e., only the dominant mode is retained.

The nominal reduced order plant model is the design model G_0 while the nominal plant model is $\hat{G}_0$. Figure 4 shows the step-responses of $\hat{G}_0$ in continuous lines against those corresponding to G_0 in dotted lines. For purposes of comparison, those corresponding to $\hat{G}_1$ (dashed) and $\hat{G}_2$ (mixed) are plotted on the same graphs.

Due to the lower order approximation, model inaccuracy is unavoidable. As the high frequency dynamics are no longer modeled, there is a significant difference between the identified model and the reduced order model. Figure 5 shows the Bode plots corresponding to the multiplicative-errors relating the design model G_0

to $\hat{G}_0$ (continuous), $\hat{G}_1$ (dotted) and $\hat{G}_2$ (dashed), respectively.

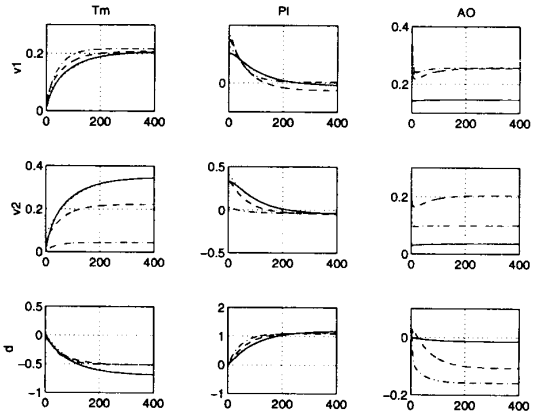

Figure 4: Step-responses of $\hat{G}_0$, G_0, $\hat{G}_1$ and $\hat{G}_2$

4.2 Uncertainty Description

As the controller must stabilize the actual plant, the robust control design methodology should take the discrepancy between model and reality into account. A standard approach is to design a controller stabilizing the nominal model in the presence of modeling errors.

A multiplicative-error is used to provide a description of the plant mismatch as well as a characterization of robust stability.

Consider the identified plant model (4) and rewrite it as follows:

$$\begin{pmatrix} y_1(t) \\ y_2(t) \end{pmatrix} = \underbrace{\begin{pmatrix} G_{1v} & G_{1d} \\ G_{2v} & G_{2d} \end{pmatrix}}_{G_0} \begin{pmatrix} v(t) \\ d(t) \end{pmatrix} \tag{5}$$

where y_1 denotes the controlled outputs and y_2 is an auxiliary output:

$$y_1(t) = \begin{pmatrix} T_m(t) \\ AO(t) \end{pmatrix} \text{ and } y_2(t) = P_I(t)$$

The plant model description corresponding to the identified model $\hat{G}_0$ is obtained by replacing G with $\hat{G}$ in (5).

Given a nominal model G_{1v} as well as the weighting function W_m, the multiplicative model set is defined as:

$$\Sigma(G_{1v}, W_m) = \{G_{1v}(I + \Delta_m W_m) \mid \Delta_m \text{stable}, \|\Delta_m\|_\infty \leq 1\}$$

where $\|\cdot\|_\infty = \max_\omega \overline{\sigma}(\cdot)$.

The **Robust Stability** criterion is defined as follows:

$$\min_K \|W_m\, T_i\|_\infty \tag{6}$$

where T_i is the plant input complementary sensitivity function, W_m is the multiplicative uncertainty weight specifying the amount of uncertainty in the model as a function of frequency, and K represents a stabilizing controller.

In the present case, the uncertainty weight is of the form $W_m = w_m I_2$, where w_m is a stable minimum-phase scalar valued function and has a large magnitude in the frequency range where the modeling error is too large; w_m is chosen as follows:

- In the frequency range where known dynamics have been neglected,

$$|w_m| \geq \|G_{1v}^{-1}(\hat{G}_{1v} - G_{1v})\|_2 \tag{7}$$

  where $\|.\|_2 = \overline{\sigma}(.)$ denotes the maximum singular value of a matrix. Outside the frequency range of the experiment, $|w_m|$ is large to account for unmodelled dynamics.
- In the frequency range where the model is accurate, $|w_m|$ is chosen to account for nonlinearities in the physical plant.

Figure 5 shows w_m (continuous) and the relative modeling errors (7) relating G_0 to $\hat{G}_0$ (continuous), $\hat{G}_1$ (dotted) and $\hat{G}_2$ (dashed), respectively.

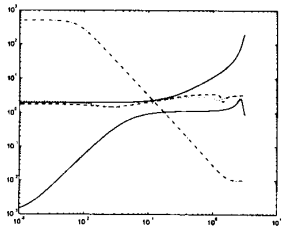

Figure 5: Uncertainty - Performance Weights and Relative errors relating G_0 to $\hat{G}_0$, $\hat{G}_1$, $\hat{G}_2$, respectively.

4.3 Performance Specifications

Consider the generalized system depicted in Figure 6. Note the design model includes the actuator dynamics, modeled by two integrators; the vertical positions of the control rods are measured.

The selection of w and z is based on performance requirements: the exogenous input w contains a disturbance input *dist* on the output, a perturbation *pert* on the control and the actual disturbance d, whereas the error signals z are weighted outputs.

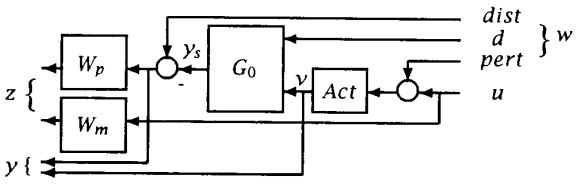

Figure 6: Generalized Model P

The **Nominal Performance** criterion is defined as follows:

$$\min_K \|W_p\, S_o\|_\infty \tag{8}$$

where S_o denotes the plant output sensitivity function and the weighting matrix W_p reflecting the performance specifications is given as follows:

$$W_p = \begin{pmatrix} w_1(j\omega) & & 0 \\ & w_2 & \\ & & \ddots \\ 0 & & w_5 \end{pmatrix}$$

The main control objective is to reject the disturbances on the temperature and to track the reference, noted T_{ref}. Note the reference is the first component of *dist*. Thus, the weighting function w_1 on the tracking error needs to be an integral action to provide a zero steady-state error and a rejection of stepwise disturbances on the temperature. Figure 5 shows the performance weight w_1 in mixed lines.

As a second objective, the control strategy should minimize the effect of the control on the axial offset. A constant weight w_2 is introduced on the axial offset. Then, the use of u_2 is preferred as it has more authority at low power and results in lower axial offset.

To limit the magnitude of the positions of the control rods, two constant weights are used, in particular w_4 and w_5 are chosen to be equal.

4.4 $\mathcal{H}_\infty$ Control Design

Consider the standard feedback system shown in Figure 7, where K is the controller and P is the generalized plant. The objective is to minimize over all frequencies the maximal energy captured by the closed-loop transfer function from exogenous inputs w to the error signal z. This transfer function is also referred as the lower linear fractional transformation and commonly noted $F_l(P,K)$. The synthesis problem involves finding a controller K such that performance requirements are satisfied under prescribed uncertainties.

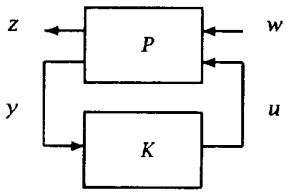

Figure 7: Feedback Interconnection of P and K

For the $\mathcal{H}_\infty$ optimal problem, the objective is to find a stabilizing controller K which minimizes $\|F_l(P,K)\|_\infty$. Thus, find a controller K such that

$$\|F_l(P,K)\|_\infty < \gamma \tag{9}$$

where $\frac{1}{\gamma}$ is the minimum norm of the perturbation that destabilizes the closed-loop system. The minimization is carried out iteratively and is known as γ-iterations [6].

4.5 Robustness Analysis

The $\mathcal{H}_\infty$ design is analyzed with respect to structured uncertainty using μ [7]. The upper and lower bounds for μ are calculated on the 7x7 closed-loop response of $F_l(P,K)$ using the following structure:

$$\Delta = \left\{ \begin{bmatrix} \Delta_m & \\ & \Delta_p \end{bmatrix} : \Delta_m \in C^{2x2}, \Delta_p \in S_p \right\}$$

and

$$S_p = \left\{ \begin{bmatrix} \Delta_1 & \\ & \Delta_2 \end{bmatrix} : \Delta_1 \in C^{3x3},\ \Delta_2 \in C^{2x2} \right\}$$

where the Δ_m and Δ_p blocks consist of an uncertainty block and two performance blocks, respectively.

The bounds for μ are plotted in Figure 8 in continuous lines (they lie on top of one another) along with the maximum singular value in dotted lines. Furthermore, the maximum singular values for robust stability (dashed) and nominal performance (mixed) as defined in (6) and (8) are shown in the same plot.

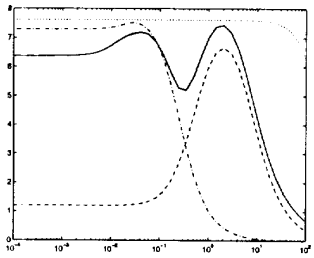

Figure 8: μ bounds and Maximum Singular Values for Robust Stability-Nominal Performance

Since the system has fewer degrees of freedom than inputs, it is only possible to minimize the axial offset, not reject it.

4.6 Simulation Results

Figure 9 shows the step-responses of the control system. Input-output signals corresponding to the nominal plant model $\hat{G}_0$ are plotted in continuous lines while those resulting from the perturbed plant models $\hat{G}_1$ and $\hat{G}_2$ are displayed in dashed and dotted lines, respectively. The external signals are plotted in mixed lines. Note that both control signals are shown in the same plot (the "smallest" one in magnitude is u_1).

The results show that the nominal performance is achieved at 50%Pn. Then, as the power is increased, the performance on the axial offset is relaxed; close to the nominal power the specifications are no longer satisfied. This type of behavior is typical on the actual plant. It emphasizes the necessity of a nonlinear controller or a gain scheduled controller to recover the performances in a wider operating range. Indeed, these results need to be validated on the simulator. Unfortunately, at the time of this study, it was not possible to test the controller on it.

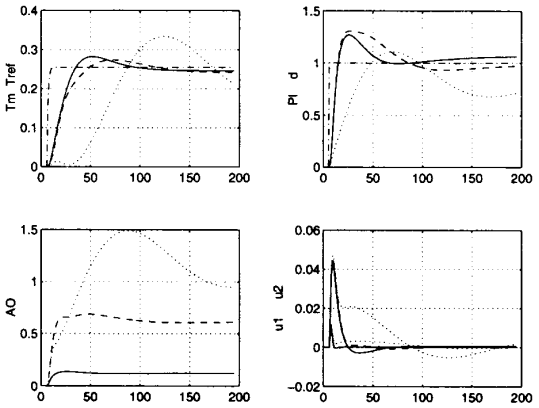

Figure 9: Closed-loop responses of $\hat{G}_0$, $\hat{G}_1$ and $\hat{G}_2$

5 Conclusion

The purpose of this study was to assess the effectiveness of an $\mathcal{H}_\infty$ controller based on a low-order model to control a pressurized water reactor. Of particular importance, the physical system was identified from experimental data using a MIMO identification-oriented state-space realization. The resulting model has been reduced using a frequency-weighted balanced realization technique. An attractive feature of the methodology is that the unmodelled dynamics of the actual system are explicitly addressed in the controller design.

The linear simulations of the closed-loop system in the presence of modeling errors demonstrate that robust performance is almost achieved up to $90\%P_n$. As the actual plant is highly nonlinear close to the nominal power, a nonlinear controller or a gain scheduled controller is required. Finally, while these results are promising, they need to be validated on a realistic nonlinear simulator.

Acknowledgements

The first author gratefully acknowledges support for this work provided by Ministère de la Recherche et de l'Espace (MRE) and by the Division of Engineering and Applied Science at Caltech. Note that this work was originally started at Electricité de France (EDF), Direction des Etudes et Recherches in Clamart, France.

References

[1] Bendotti, P. and E. Irving,"Design of an $\mathcal{H}_2$ Controller for a Pressurized Water Reactor", *Proc. of the IFAC Symposium on Robust Control Design*, Rio, Brazil, Sept. 1994.

[2] Bendotti, P. and E. Irving, "Modeling and Robust Frequency-shaped LQG Control of a Pressurized Water Reactor", *Internal Note, EDF HI/20/93/009*, August 1993.

[3] Ljung, L., *System Identification - Theory for the User*, Prentice-Hall, Englewood Cliffs, N. J., (1987).

[4] Moore, B., "Principal Component Analysis in Linear Systems: Controllability, Observability, and Model Reduction", *IEEE Trans. Automatic Control*, Vol. AC-26, pp. 17-31, 1981.

[5] Enns, D. F., "Model Reduction with Balanced Realizations: an Error Bound and a frequency Weighted Generalization", *Proc. of IEEE Conf. on Decision and Control*, Vol. 2, pp. 127-132, 1984.

[6] Doyle, J. C., K. Glover, P. P. Khargonekar and B. Francis, "State-space Solutions to Standard $\mathcal{H}_2$ and $\mathcal{H}_\infty$ Control Problems", *IEEE Trans. Automatic Control*,Vol. AC-34, No. 1, pp. 831-847, 1989.

[7] Packard, A., and J. Doyle, "The Complex Structured Singular Value", *Automatica*, Vol. 29, No. 1, 1993, pp. 71-109.